NASA Technical Memorandum 85750

Potential Flow Through a Cascade of Alternately Displaced Circular Bodies—The Rod-Wall Wind-Tunnel Boundary Condition

Joel L. Everhart

MARCH 1984

NASA

NASA Technical Memorandum 85750

Potential Flow Through a Cascade of Alternately Displaced Circular Bodies—The Rod-Wall Wind-Tunnel Boundary Condition

Joel L. Everhart
Langley Research Center
Hampton, Virginia

National Aeronautics
and Space Administration

Scientific and Technical
Information Office

1984

SUMMARY

An approximate solution for the potential flow through a cascade consisting of two rows of staggered circular rods is derived. The solution is then used to obtain the classic slotted-wall boundary-condition coefficient applicable to rod-wall wind tunnels. A comparison with the solution of Chen and Mears (as corrected by Barnwell) for flow through an unstaggered cascade is also made.

INTRODUCTION

Longitudinally slotted wind-tunnel test sections which have slat shapes with circular cross sections are generally referred to as rod-wall wind tunnels. Figure 1(a) shows the side view of the wind-tunnel flow expanding around the model and going through the wall into the plenum surrounding the test section. Figure 1(b) gives a cross-sectional view of the rod elements and defines the pertinent geometric parameters.

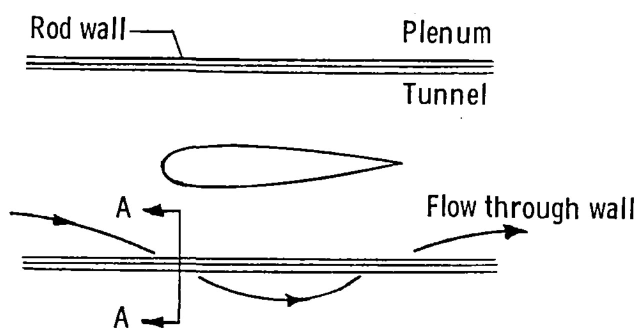

(a) Side view of rod-wall wind tunnel.

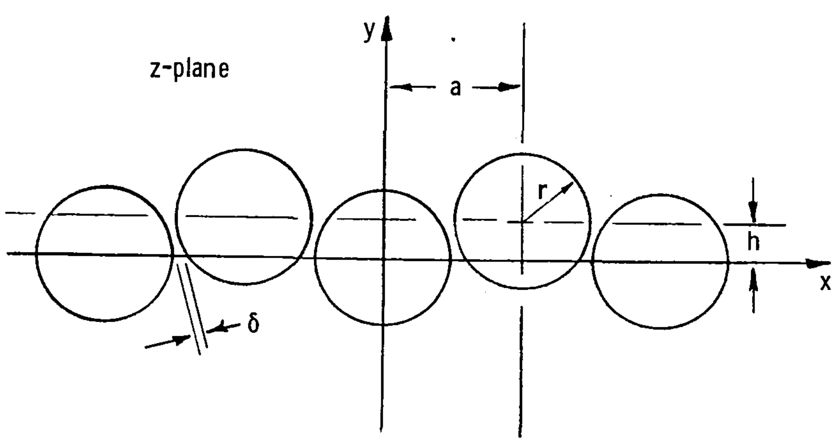

(b) Cross section A-A. End view of rod wall.

Figure 1.- Diagram of rod-wall wind tunnel.

In 1952, Sabol (ref. 1) published the ballistic range results of a study of the shock reflection properties of walls with various slat cross-sectional shapes (including circular) in both circular and rectangular test sections. His studies indicated that reflected shock waves of sharply reduced strength occurred when the walls had faired slots. In 1974, Binion and Anderson (ref. 2) compared acoustic data and aerodynamic data taken in both rod-wall and perforated-wall wind tunnels at transonic speeds. They found that the rod walls had lower noise levels than the perforated walls and that the aerodynamic data were as good as, or better than, the perforated-wall results. Gilliam (ref. 3) extended the transonic rod-wall acoustics study of reference 2 and found this type of wall to be very quiet in comparison with other transonic tunnels. His results also indicated that the subsonic fluctuating pressure coefficient approached that of a solid-wall wind tunnel with a turbulent wall boundary layer. Harvey et al. (ref. 4) examined the effect of rod gap width on noise attenuation as well as on wall boundary-layer removal and laminarization in supersonic tunnels. They were able to correlate the transition Reynolds number with gap width and to show that laminar rod-wall boundary layers introduced insignificant noise into the flow field. Recently, Harney et al. (ref. 5) published a paper citing their work on a transonic, adaptive rod-wall wind tunnel; it had solid sidewalls with upper and lower rod walls with both longitudinal and spanwise wall-jacking stations. This configuration allowed two-dimensional and some three-dimensional wall adaptation through changes in the wall openness ratio or changes in the wall shape or both to match free air streamlines about the model.

The purpose of this report is to obtain an approximate, homogeneous rod-wall boundary condition. First, a solution for the inviscid, incompressible cross flow through a rod wall composed of alternately staggered rods is obtained by linear superposition of doublet singularities. After constructing this solution, it is then possible, using the method outlined by Barnwell (ref. 6), to obtain a classic homogeneous slotted-wall-type boundary condition for the rod wall. This solution differs from that of Chen and Mears (ref. 7) in that their solution did not allow for off-axis movement of the rods.

SYMBOLS

a	slot spacing (horizontal displacement between adjacent rods)
c_1	doublet strength coefficient
c_2	doublet-rod strength coefficient
F	complex potential functions
h	vertical displacement of adjacent rods
Im( )	imaginary part of ( )
i	imaginary number, $\sqrt{-1}$
K	slotted-wall boundary-condition coefficient
Re( )	real part of ( )

r	rod radius
U	horizontal cross-flow velocity
V	vertical cross-flow velocity
V_a	vertical cross-flow velocity far from the rods (i.e., the tunnel ambient component)
W	complex velocity, $U - iV$
x,y	cross-flow coordinates (see fig. 1(b))
x',y'	coordinates in z'-plane (see fig. 2(a))
x_a,x_b	starting and ending locations of doublet rod
x_g,y_g	coordinates for gap point
y_d	vertical distance from rod center to isolated doublet
y_s	stagnation point
z	complex variable, $x + iy$
z'	intermediate complex variable, $x' + iy'$
α,β	angles of inclination between doublet axis and x-axis
δ	slot width
θ	angle of inclination between doublet axis and y-axis
λ_i	transformation variable, $i = 1, 2, 3, 4$
μ	doublet strength
μ_1	strength of isolated doublet
μ_2	strength of doublet rod per unit length
Φ	complex rod-wall potential, $\phi + i\psi$
Φ_r	nondimensional rapidly varying potential
ϕ	velocity potential
ϕ_o	velocity potential used to enforce far-field boundary condition
ϕ_r	rapidly varying portion of velocity potential
ψ	stream function

FORMULATION AND ANALYSIS

The problem presented herein is to suitably approximate the inviscid cross flow through a cascade of circular bodies as shown in figure 1(b). The potential is constructed by adding combinations of elementary solutions of the Laplace equation which satisfy the boundary conditions at specific locations. It is assumed that no lift is generated; that is, the flow does not separate. Since the bodies are closed, only doublet singularities are needed.

The complex potential of a doublet singularity at the origin of the z'-plane is given by

$$F(z') = -\frac{\mu e^{i\alpha}}{z'} \tag{1}$$

If a row of doublets is placed at $z' = 0, \pm 2a, \ldots, \pm 2na, \ldots$ we have

$$F(z') = -\mu e^{i\alpha}\left[\frac{1}{z'} + \sum_{n=1}^{\infty}\left(\frac{1}{z' + 2na} + \frac{1}{z' - 2na}\right)\right]$$

Letting $\lambda_1 = z'/a$ and using expression (830) of reference 8 gives

$$F(\lambda_1) = -\frac{\mu e^{i\alpha}\pi}{2a}\cot\left(\frac{\pi\lambda_1}{2}\right)$$

Thus,

$$F(z') = -\frac{\mu e^{i\alpha}\pi}{2a}\cot\left(\frac{\pi z'}{2a}\right) \tag{2}$$

If rows of doublets are placed at $z' = z - iy_d$ and $z' = z + a - i(h - y_d)$, then, from equation (2), the complex potential of the combined doublet rows in the z-plane is expressed as

$$F(z) = -\frac{i\mu_1\pi}{a}\,\frac{\cos\frac{\pi}{a}\left(z - i\,\frac{h}{2}\right)}{\sin\frac{\pi}{a}\left(z - i\,\frac{h}{2}\right) + i\,\sinh\frac{\pi}{a}\left(\frac{h}{2} - y_d\right)} \tag{3}$$

where μ_1 represents the strength of each of the individual doublets and $\alpha = \pi/2$, which aligns the doublet axes with the oncoming flow through the wall.

Now let equation (1) be the elemental potential of a continuous, constant-strength distribution of doublets, that is, $\mu = \mu_2 \, dx'$. It can be seen by referring to figure 2(a) that

$$
\begin{aligned}
F(z') &= -\mu_2 e^{i\alpha} \int_{-x_b}^{-x_a} \frac{dx'}{z' - x'} - \mu_2 e^{i\beta} \int_{x_a}^{x_b} \frac{dx'}{z' - x'} \\
&= \mu_2 e^{i\alpha} \ln\left(\frac{z' + x_a}{z' + x_b}\right) + \mu_2 e^{i\beta} \ln\left(\frac{z' - x_b}{z' - x_a}\right) \qquad (4)
\end{aligned}
$$

where $\alpha = (\pi/2) + \theta$ and $\beta = (\pi/2) - \theta$. If an infinite row of doublet-rod pairs are placed at z', $z' \pm 2a$, ..., then

$$
\begin{aligned}
F(z') = \mu_2 e^{i\alpha} &\ln\left[\left(\frac{z' + x_a}{z' + x_b}\right)\left(\frac{z' + 2a + x_a}{z' + 2a + x_b}\right)\left(\frac{z' - 2a + x_a}{z' - 2a + x_b}\right) \cdots\right] \\
+ \mu_2 e^{i\beta} &\ln\left[\left(\frac{z' - x_b}{z' - x_a}\right)\left(\frac{z' + 2a - x_b}{z' + 2a - x_a}\right)\left(\frac{z' - 2a - x_b}{z' - 2a - x_a}\right) \cdots\right]
\end{aligned}
$$

Alternately, by letting

$$\lambda_1 = \frac{\pi}{2} \frac{z' + x_a}{a}$$

$$\lambda_2 = \frac{\pi}{2} \frac{z' + x_b}{a}$$

$$\lambda_3 = \frac{\pi}{2} \frac{z' - x_b}{a}$$

$$\lambda_4 = \frac{\pi}{2} \frac{z' - x_a}{a}$$

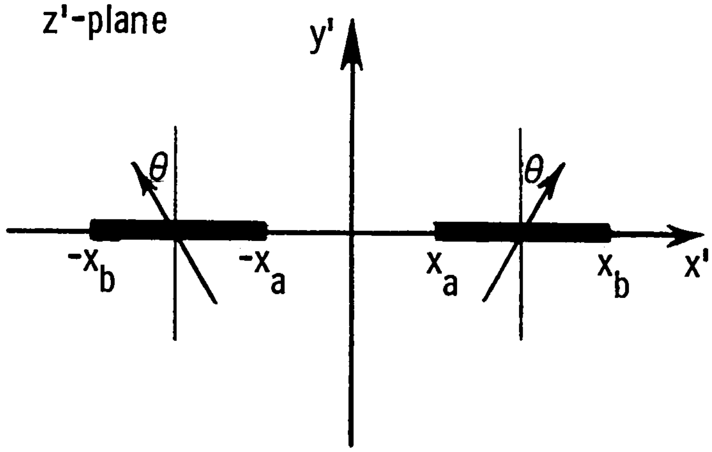

(a) Doublet rods in z'-plane.

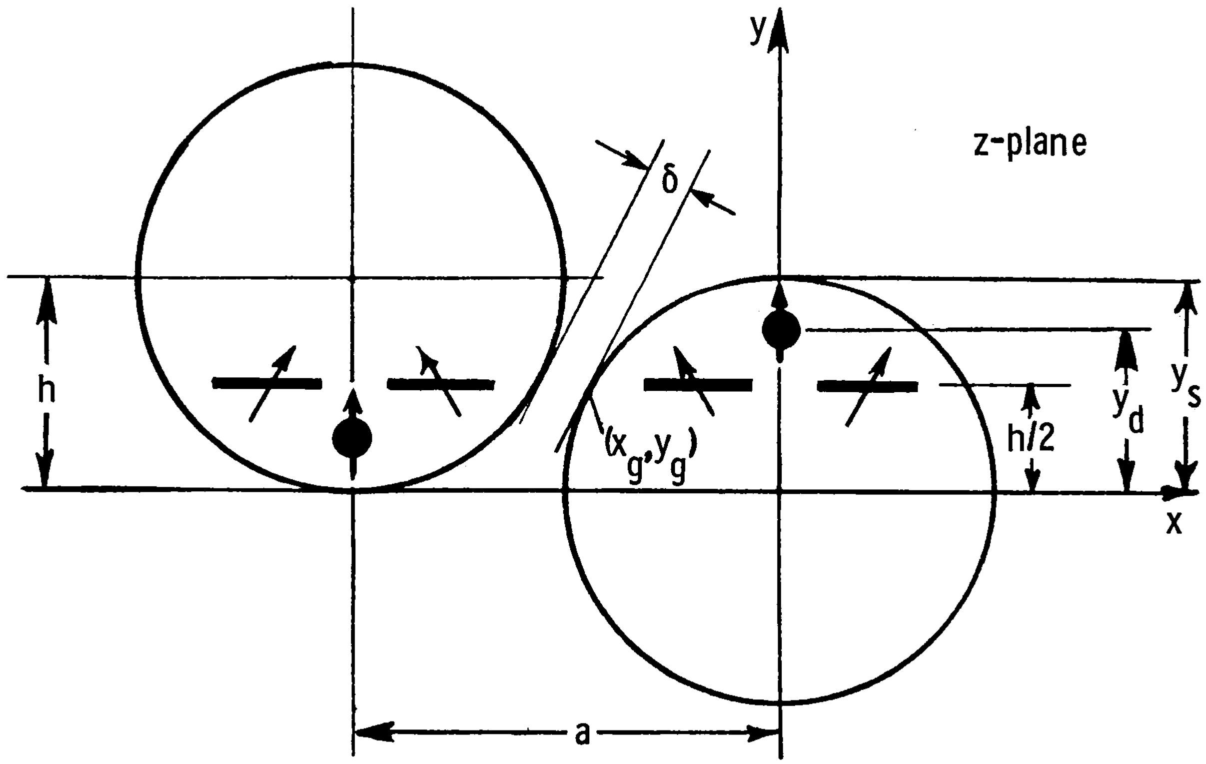

(b) Distributed singularities in z-plane.

Figure 2.- Singularity distribution used for modeling the rod-wall boundary condition.

the complex potential function becomes

$$F(\lambda_1,\lambda_2,\lambda_3,\lambda_4) = \mu_2 e^{i\alpha} \ln\left[\frac{\frac{2a}{\pi}\lambda_1 \cdots \left(\frac{2a}{\pi}\right)^2\left(1 - \frac{\lambda_1^2}{n^2\pi^2}\right) \cdots}{\frac{2a}{\pi}\lambda_2 \cdots \left(\frac{2a}{\pi}\right)^2\left(1 - \frac{\lambda_2^2}{n^2\pi^2}\right) \cdots}\right]$$

$$+ \mu_2 e^{i\beta} \ln\left[\frac{\frac{2a}{\pi}\lambda_3 \cdots \left(\frac{2a}{\pi}\right)^2\left(1 - \frac{\lambda_3^2}{n^2\pi^2}\right) \cdots}{\frac{2a}{\pi}\lambda_4 \cdots \left(\frac{2a}{\pi}\right)^2\left(1 - \frac{\lambda_4^2}{n^2\pi^2}\right) \cdots}\right]$$

$$= \mu_2 e^{i\alpha} \ln\left(\frac{\sin \lambda_1}{\sin \lambda_2}\right) + \mu_2 e^{i\beta} \ln\left(\frac{\sin \lambda_3}{\sin \lambda_4}\right)$$

after using expression (1016) of reference 8. Thus,

$$F(z') = \mu_2 e^{i\alpha} \ln\left[\frac{\sin \frac{\pi}{2a}(z' + x_a)}{\sin \frac{\pi}{2a}(z' + x_b)}\right] + \mu_2 e^{i\beta} \ln\left[\frac{\sin \frac{\pi}{2a}(z' - x_b)}{\sin \frac{\pi}{2a}(z' - x_a)}\right] \tag{5}$$

The doublet-rod pairs defined by equation (5) are next placed at $z' = z - i(h/2)$ along with their images, which are placed at $z - i(h/2) + a$. The combination of equation (5) plus its images is given by

$$F(z) = \mu_2 e^{i\alpha} \ln\left[\frac{\sin \frac{\pi}{2a}\left(z + x_a - i\frac{h}{2}\right)}{\sin \frac{\pi}{2a}\left(z + x_b - i\frac{h}{2}\right)} \frac{\sin \frac{\pi}{2a}\left(z - x_b - i\frac{h}{2} + a\right)}{\sin \frac{\pi}{2a}\left(z - x_a - i\frac{h}{2} + a\right)}\right]$$

$$+ \mu_2 e^{i\beta} \ln\left[\frac{\sin \frac{\pi}{2a}\left(z - x_b - i\frac{h}{2}\right)}{\sin \frac{\pi}{2a}\left(z - x_a - i\frac{h}{2}\right)} \frac{\sin \frac{\pi}{2a}\left(z + x_a - i\frac{h}{2} + a\right)}{\sin \frac{\pi}{2a}\left(z + x_b - i\frac{h}{2} + a\right)}\right] \tag{6}$$

The complex potential of a free stream along the imaginary axis is given by

$$F(z) = iV_a z \tag{7}$$

We can define

$$c_1 = \mu_1/V_a \tag{8a}$$

$$c_2 = \mu_2/V_a \tag{8b}$$

$$\Phi = F/V_a \tag{8c}$$

and then add equations (3), (6), and (7) and simplify to obtain

$$\begin{aligned}
\Phi(z) = iz &- i\,\frac{\pi c_1}{a}\,\frac{\cos\frac{\pi}{a}\left(z - i\,\frac{h}{2}\right)}{\sin\frac{\pi}{a}\left(z - i\,\frac{h}{2}\right) + i\sinh\frac{\pi}{a}\left(\frac{h}{2} - y_d\right)} \\
&+ c_2\sin\theta\left\{\ln\left[\frac{-\cos\frac{\pi}{a}\left(z - i\,\frac{h}{2}\right) + \cos\frac{\pi x_b}{a}}{\cos\frac{\pi}{a}\left(z - i\,\frac{h}{2}\right) + \cos\frac{\pi x_b}{a}}\right]\right. \\
&\left. - \ln\left[\frac{-\cos\frac{\pi}{a}\left(z - i\,\frac{h}{2}\right) + \cos\frac{\pi x_a}{a}}{\cos\frac{\pi}{a}\left(z - i\,\frac{h}{2}\right) + \cos\frac{\pi x_a}{a}}\right]\right\} \\
&+ ic_2\cos\theta\left\{\ln\left[\frac{\sin\frac{\pi}{a}\left(z - i\,\frac{h}{2} - x_b\right)}{\sin\frac{\pi}{a}\left(z - i\,\frac{h}{2} + x_b\right)}\right]\right. \\
&\left. - \ln\left[\frac{\sin\frac{\pi}{a}\left(z - i\,\frac{h}{2} - x_a\right)}{\sin\frac{\pi}{a}\left(z - i\,\frac{h}{2} + x_a\right)}\right]\right\}
\end{aligned} \tag{9}$$

The resulting system of singularities is as shown in figure 2(b). Equation (9) represents the complex potential of a cascade consisting of two staggered rows of closed bodies whose shapes are determined by choosing c_1, c_2, h, y_d, x_a, and x_b. The complex velocity W is obtained by differentiating equation (9), which gives the following:

$$W(z) = \frac{d\Phi}{dz} = i + i\left(\frac{\pi}{a}\right)^2 c_1 \left\{ \frac{1 + i \sin \frac{\pi}{a}\left(z - i\frac{h}{2}\right) \sinh \frac{\pi}{a}\left(\frac{h}{2} - y_d\right)}{\left[\sin \frac{\pi}{a}\left(z - i\frac{h}{2}\right) + i \sinh \frac{\pi}{a}\left(\frac{h}{2} - y_d\right)\right]^2} \right\}$$

$$+ \frac{\pi}{a} c_2 \sin\theta \left[\frac{\sin \frac{\pi}{a}\left(z - i\frac{h}{2}\right)}{-\cos \frac{\pi}{a}\left(z - i\frac{h}{2}\right) + \cos \frac{\pi x_b}{a}} + \frac{\sin \frac{\pi}{a}\left(z - i\frac{h}{2}\right)}{\cos \frac{\pi}{a}\left(z - i\frac{h}{2}\right) + \cos \frac{\pi x_b}{a}} \right.$$

$$\left. - \frac{\sin \frac{\pi}{a}\left(z - i\frac{h}{2}\right)}{-\cos \frac{\pi}{a}\left(z - i\frac{h}{2}\right) + \cos \frac{\pi x_a}{a}} - \frac{\sin \frac{\pi}{a}\left(z - i\frac{h}{2}\right)}{\cos \frac{\pi}{a}\left(z - i\frac{h}{2}\right) + \cos \frac{\pi x_a}{a}} \right]$$

$$+ i\frac{\pi}{a} c_2 \cos\theta \left[\cot \frac{\pi}{a}\left(z - i\frac{h}{2} - x_b\right) - \cot \frac{\pi}{a}\left(z - i\frac{h}{2} + x_b\right) \right.$$

$$\left. - \cot \frac{\pi}{a}\left(z - i\frac{h}{2} - x_a\right) + \cot \frac{\pi}{a}\left(z - i\frac{h}{2} + x_a\right) \right] \qquad (10)$$

The stream and potential functions may be obtained by taking the real and imaginary portions of equation (9). The velocity components may be obtained from the real and imaginary portions of equation (10). Thus,

$$\phi = \mathrm{Re}(\Phi) \qquad (11a)$$

$$\psi = \mathrm{Im}(\Phi) \qquad (11b)$$

$$U = \mathrm{Re}(W) \qquad (11c)$$

$$V = -\mathrm{Im}(W) \qquad (11d)$$

which give the following:

$$\phi = -y + c_1 A_{12} + c_2 \left[\sin\theta\,(A_{21} - A_{31}) + \cos\theta\,(A_{52} - A_{42})\right] \tag{12}$$

$$\psi = x - c_1 A_{11} + c_2 \left[\sin\theta\,(A_{22} - A_{32}) + \cos\theta\,(A_{41} - A_{51})\right] \tag{13}$$

$$U\Big|_{z=iy_s} = 0 \tag{14}$$

$$V\Big|_{z=iy_s} = -1 + c_1 A_{62} - c_2 \left[\sin\theta\,(A_{72} - A_{82}) + \cos\theta\,(A_{92} - A_{102})\right] = 0 \tag{15}$$

where the A_{ij} coefficients are defined in the appendix and y_s is the stagnation point. The problem is to now find or specify values of θ, c_1, c_2, y_d, h/d, x_a, and x_b such that the desired rod shape is reasonably approximated.

HOMOGENEOUS BOUNDARY CONDITION

The classic form of the homogeneous boundary condition is

$$\frac{\partial\phi}{\partial x} + aK\,\frac{\partial^2\phi}{\partial x\,\partial y} = 0 \tag{16}$$

where K is the boundary-condition coefficient for a specified wall geometry. With Barnwell's method (ref. 6), K may be easily obtained once the potential is derived. Since solutions to Laplace's equation are correct to within an additive constant, equation (12) is written as

$$\phi = -y + \phi_r + \phi_o \tag{17}$$

where ϕ_r is the rapidly varying portion of the potential in the vicinity of the wall and ϕ_o is an additive constant which forces the boundary condition

$$\lim_{y\to\infty} \phi_r = 0 \tag{18}$$

to hold. Thus,

$$\lim_{y\to\infty} \phi_r = \lim_{y\to\infty}(\phi + y - \phi_o) = 0 \tag{19}$$

giving

$$\phi_o = -\frac{\pi}{a}\left[c_1 + 2c_2(x_b - x_a)\cos\theta\right] \tag{20}$$

From equation (20), it follows that

$$\phi_r = c_1\left(A_{12} + \frac{\pi}{a}\right) + c_2\left[\sin\theta\,(A_{21} - A_{31}) + \cos\theta\,(A_{52} - A_{42}) + \frac{2\pi}{a}(x_b - x_a)\cos\theta\right] \tag{21}$$

Equation (21) may be written as

$$\phi_r = a\Phi_r \tag{22}$$

Evaluating Φ_r in the slot gives the desired result; that is,

$$K = \Phi_r \qquad (x = a/2;\quad y = h/2) \tag{23}$$

or

$$K = \frac{\pi}{a^2}\left[c_1 + 2c_2(x_b - x_a)\cos\theta\right] \tag{24}$$

As a check on the solution, equation (15) was compared with the Chen and Mears solution (ref. 7) as corrected by Barnwell (ref. 6). Chen and Mears used a doublet-rod model similar to what is presented here; however, their solution did not allow for the off-axis displacement of the alternate wall members. If c_1, x_a, θ, and h are set to zero, then equation (15) reduces to the corrected Chen and Mears solution.

METHOD OF SOLUTION

The equations which must be solved are given by equations (13), (15), and (24). The unknowns are x_a, x_b, c_1, c_2, θ, y_d, and K, with parameters h, r, and a. To reduce the number of unknowns, x_a is arbitrarily set to 0.01 for cases when $h \neq 0$ and to 0 for cases when the rods are aligned. The rod length x_b is determined such that the zero streamline (eq. (13)) is forced through a point in the gap with the coordinates

$$y_g = h/2 \tag{25a}$$

$$x_g = (y_s^2 - y_g^2)^{1/2} \tag{25b}$$

It should be noted that the rod radius r sets the stagnation point y_s at x equal to zero. The doublet strength c_1 is determined such that equation (15) is satisfied at the upper stagnation point $(0,y_s)$, and the doublet-rod strength c_2 is determined such that equation (15) is satisfied at the lower stagnation point $(0,-y_s)$.

In reference 6 it was shown that K was very dependent on the slot radius of curvature. Therefore, θ is determined so that the radius of curvature in the gap is equal to r. The doublet position y_d is set so as to minimize the root-mean-square (rms) deviation from a circular body of radius r. The boundary-condition coefficient K is calculated from equation (24).

The solution procedure is iterative and, in many cases, the convergence is highly sensitive to the initial choice of variables. The gap point (x_g,y_g) where the radius of curvature is specified is not the point of minimum separation between the displaced cylinders. However, for small values of h, it is sufficiently accurate. If the minimum-separation point is used, instability develops in the solution procedure and, for the larger wall openness values, undesirable body shapes are obtained.

RESULTS

Wall openness δ/a as a function of rod displacement h/a is given by the expression

$$\frac{\delta}{a} = \left[1 + \left(\frac{h}{a}\right)^2\right]^{1/2} - 2\,\frac{r}{a} \tag{26}$$

and is plotted for a rod radius of $a/2$ in figure 3. Body shapes for various values of wall openness and a fixed radius r of $a/2$ are shown in figure 4. These shapes were determined from equation (13) by solving for the zero streamline. The maximum rms error from a circular body for $0 < h/a < 0.90$ was 0.0070, which occurred at $h/a = 0.45$. Typical rms values, however, were of the order of 0.0040. For those cases in which the rods were not offset, the openness was changed by varying r; the rms error decreased with increasing wall openness, going from 0.005 at 0.6-percent open to less than 0.001 at 30.0-percent open.

In the present study, the rod radius and the radius of curvature matched in the gap between the doublet rods at the point (x_g,y_g) as opposed to matching in the slot at the minimum. For openness ratios less than 10 percent, the difference in location between the minimum and the gap are insignificant. For openness ratios greater than 10 percent, the difference can be substantial. Barnwell (ref. 6) showed large changes in the boundary-condition coefficient K with varying radius of curvature when the wall openness ratio was small. Large changes also occur with varying openness ratio and fixed curvature. During the present study it was found that these two parameters controlled the value of K for small openness ratios even more than the actual rod cross-sectional shape. For large openness ratios, the major effect is

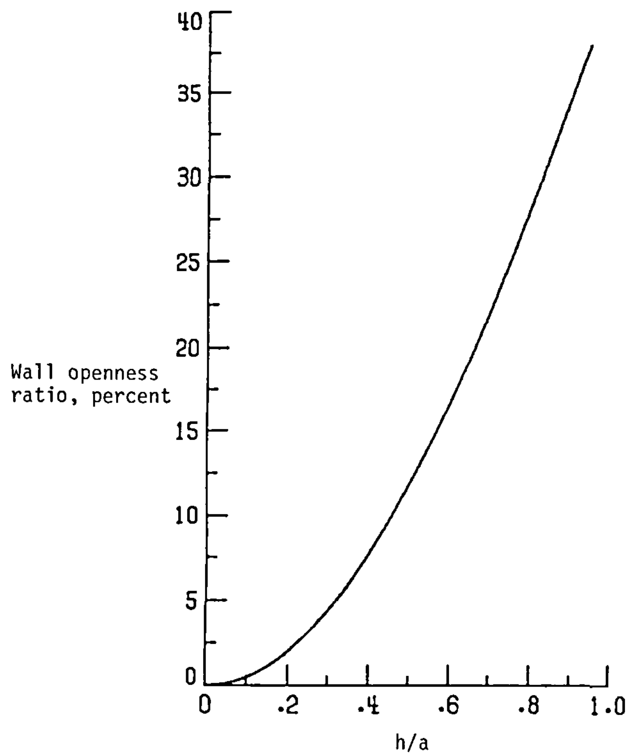

Figure 3.- Wall openness ratio versus rod displacement for rod radius of a/2.

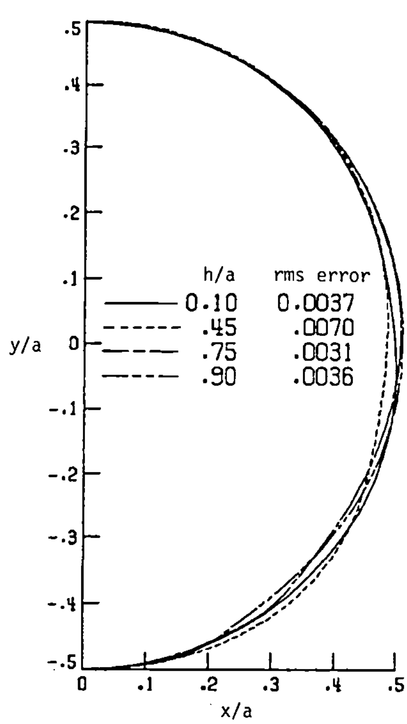

Figure 4.- Calculated body shapes for various values of h/a for rod radius of a/2.

openness ratio. Figure 5 shows a comparison between the present case of displaced rods with a radius of $a/2$ and the Chen and Mears solution for undisplaced circular rods (ref. 7). For openness ratios of less than about 12 percent, the Chen and Mears solution and the present solution are equally applicable. If the openness exceeds about 12 percent, the effect of rod displacement begins to appear and the difference between the solutions grows to a factor of about 2. It should be emphasized, however, that the applicability of the homogeneous wall boundary condition becomes suspect at these large values of openness.

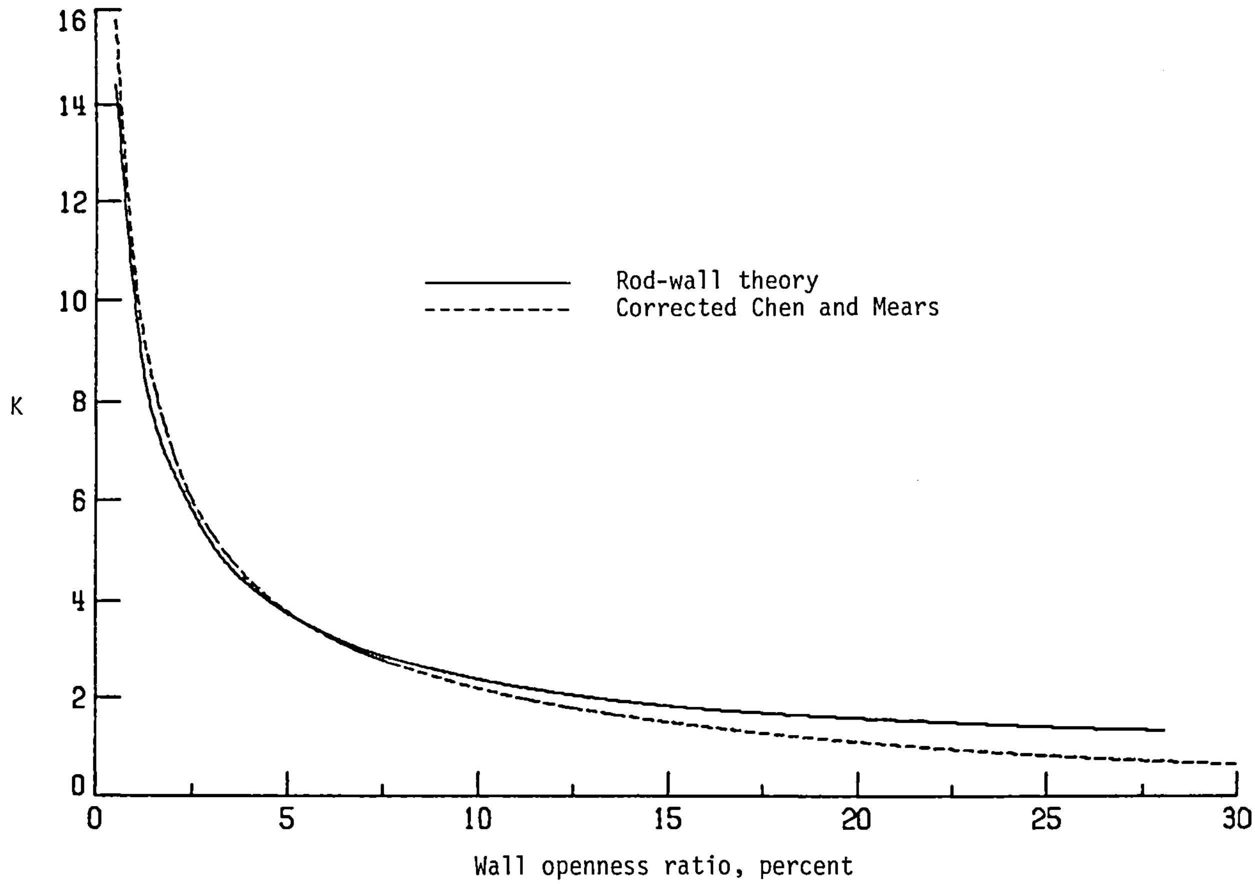

Figure 5.- Rod-wall boundary condition for cylinder of radius $a/2$.

CONCLUDING REMARKS

An approximate, two-dimensional potential flow solution for the flow through a cascade of alternately displaced circular rods has been formulated. The solution was constructed by using discrete doublet and doublet-rod singularities. Free parameters in the solution were defined by minimizing the root-mean-square error deviation between the body streamline and a circle of given radius. The radius of curvature in the gap between two adjacent bodies was also specified and matched. With a method described by Barnwell, the homogeneous slotted-wall wind-tunnel boundary-condition coefficient is derived.

For the case of undisplaced rods, the solution reduced to that of the classic Chen and Mears solution for the rod wall as corrected by Barnwell. For cases when alternate rods are displaced, the maximum root-mean-square error deviation from a circular cross section was determined as 0.0070. The boundary-condition coefficient is approximately equal to that given by the corrected Chen and Mears theory for wall openness ratio of less than about 12 percent. Values of wall openness ratio greater than this show deviations increasing to a factor of about 2.

Langley Research Center
National Aeronautics and Space Administration
Hampton, VA 23665
February 3, 1984

APPENDIX

COEFFICIENTS OF STREAM, POTENTIAL, AND VELOCITY FUNCTIONS

If we define the parameters

$$\left.\begin{aligned}
P &= \pi y_d/a \\
Q &= \pi x_a/a \\
R &= \pi x_b/a \\
s_1 &= \pi x/a \\
s_2 &= \pi(x - x_a)/a \\
s_3 &= \pi(x + x_a)/a \\
s_4 &= \pi(x - x_b)/a \\
s_5 &= \pi(x + x_b)/a \\
t_1 &= \pi[y - (h/2)]/a \\
t_2 &= \pi[(h/2) - y_d]/a
\end{aligned}\right\} \tag{A1}$$

then the A_{ij} coefficients used in equations (12) to (15) are given by the following:

$$A_{11} = \frac{\pi}{a} \frac{\frac{1}{2} \sin 2s_1 - \sinh t_2 \sin s_1 \sinh t_1}{(\sin s_1 \cosh t_1)^2 + (\cos s_1 \sinh t_1 + \sinh t_2)^2} \tag{A2}$$

$$A_{12} = -\frac{\pi}{a} \frac{\frac{1}{2} \sinh 2t_1 + \sinh t_2 \cos s_1 \cosh t_1}{(\sin s_1 \cosh t_1)^2 + (\cos s_1 \sinh t_1 + \sinh t_2)^2} \tag{A3}$$

APPENDIX

$$A_{21} = \frac{1}{2} \ln \frac{(-\cos s_1 \cosh t_1 + \cos R)^2 + (\sin s_1 \sinh t_1)^2}{(\cos s_1 \cosh t_1 + \cos R)^2 + (\sin s_1 \sinh t_1)^2} \tag{A4}$$

$$A_{22} = \tan^{-1} \frac{2 \cos R \sin s_1 \sinh t_1}{\cos^2 R - \cos^2 s_1 - \sinh^2 t_1} \tag{A5}$$

$$A_{31} = \frac{1}{2} \ln \frac{(-\cos s_1 \cosh t_1 + \cos Q)^2 + (\sin s_1 \sinh t_1)^2}{(\cos s_1 \cosh t_1 + \cos Q)^2 + (\sin s_1 \sinh t_1)^2} \tag{A6}$$

$$A_{32} = \tan^{-1} \frac{2 \cos Q \sin s_1 \sinh t_1}{\cos^2 Q - \cos^2 s_1 - \sinh^2 t_1} \tag{A7}$$

$$A_{41} = \frac{1}{2} \ln \frac{\sin^2 s_4 + \sinh^2 t_1}{\sin^2 s_5 + \sinh^2 t_1} \tag{A8}$$

$$A_{42} = \tan^{-1} \frac{\sinh 2t_1 \sin 2R}{\cos 2R \cosh 2t_1 - \cos 2s_1} \tag{A9}$$

$$A_{51} = \frac{1}{2} \ln \frac{\sin^2 s_2 + \sinh^2 t_1}{\sin^2 s_3 + \sinh^2 t_1} \tag{A10}$$

$$A_{52} = \tan^{-1} \frac{\sinh 2t_1 \sin 2Q}{\cos 2Q \cosh 2t_1 - \cos 2s_1} \tag{A11}$$

$$A_{62} = \left(\frac{\pi}{a}\right)^2 \frac{1 - \sinh \frac{\pi}{a}\left(y_s - \frac{h}{2}\right) \sinh t_2}{\left[\sinh \frac{\pi}{a}\left(y_s - \frac{h}{2}\right) + \sinh t_2\right]^2} \tag{A12}$$

$$A_{72} = \frac{\pi}{a} \frac{2 \sinh \frac{\pi}{a}\left(y_s - \frac{h}{2}\right) \cos R}{\cos^2 R - \left[\cosh^2\left(\frac{\pi}{a}\right)\right]\left(y_s - \frac{h}{2}\right)} \tag{A13}$$

$$A_{82} = \frac{\pi}{a} \frac{2 \sinh \frac{\pi}{a}\left(y_s - \frac{h}{2}\right) \cos Q}{\cos^2 Q - \left[\cosh^2\left(\frac{\pi}{a}\right)\right]\left(y_s - \frac{h}{2}\right)} \tag{A14}$$

$$A_{92} = \frac{2\pi}{a} \frac{\sin 2R}{\cos 2R - \cosh \frac{2\pi}{a}\left(y_s - \frac{h}{2}\right)} \tag{A15}$$

$$A_{102} = \frac{2\pi}{a} \frac{\sin 2Q}{\cos 2Q - \cosh \frac{2\pi}{a}\left(y_s - \frac{h}{2}\right)} \tag{A16}$$

Coefficients in equations (A1) to (A11) are obtained from equations (11a) and (11b) and coefficients in equations (A12) to (A16) are obtained by evaluating equations (11c) and (11d) at $x = 0$ and $y = y_s$, the stagnation point on the cylinder centered at $z = 0$.

REFERENCES

1. Sabol, A. P.: A Preliminary Investigation of Shock-Wave Reflections in a Small Closed Ballistic Range With Various Types of Walls. NACA RM L2G25, 1952.

2. Binion, T. W., Jr.; and Anderson, C. F.: An Experimental Investigation of the Acoustic and Wall Interference Properties of Rod and Perforated Wind Tunnel Walls in Two-Dimensional Transonic Flow. AEDC-TR-74-41, U.S. Air Force, Sept. 1974.

3. Gilliam, Fred T.: An Experimental Investigation of the Acoustic and Wave Attenuation Characteristics of a Rod Wall Wind Tunnel in Transonic Flow. AIAA Paper No. 76-215, Jan. 1976.

4. Harvey, W. D.; Stainback, P. C.; and Srokowski, A. J.: Effect of Slot Width on Transition and Noise Attenuation of a Sound Shield Panel for Supersonic Wind Tunnels. Proceedings - AIAA 9th Aerodynamic Testing Conference, June 1976, pp. 198-222.

5. Harney, D. J.; Cain, M. R.; and Ballard, B. L.: Experimental Transonic Studies of a Three-Dimensional Adaptive-Wall Wind Tunnel. Proceedings 9th Annual Mini-Symposium on Aerospace Science and Technology, AIAA, Mar. 22, 1983, pp. 7-2-1 - 7-2-6.

6. Barnwell, Richard W.: Improvements in the Slotted-Wall Boundary Condition. Proceedings - AIAA 9th Aerodynamic Testing Conference, June 1976, pp. 21-30.

7. Chen, C. F.; and Mears, J. W.: Experimental and Theoretical Study of Mean Boundary Conditions at Perforated and Longitudinally Slotted Wind Tunnel Walls. AEDC-TR-57-20, DTIC Doc. No. AD 144 320, U.S. Air Force, Dec. 1957.

8. Jolley, L. B. W., [compiler]: Summation of Series, Second rev. ed. Dover Publ., Inc., c.1961.

1. Report No.	2. Government Accession No.	3. Recipient's Catalog No.
NASA TM-85750		

4. Title and Subtitle	5. Report Date
POTENTIAL FLOW THROUGH A CASCADE OF ALTERNATELY DISPLACED CIRCULAR BODIES - THE ROD-WALL WIND-TUNNEL BOUNDARY CONDITION	March 1984
	6. Performing Organization Code 505-31-23-06
7. Author(s) Joel L. Everhart	8. Performing Organization Report No. L-15617
	10. Work Unit No.
9. Performing Organization Name and Address NASA Langley Research Center Hampton, VA 23665	11. Contract or Grant No.
	13. Type of Report and Period Covered Technical Memorandum
12. Sponsoring Agency Name and Address National Aeronautics and Space Administration Washington, DC 20546	14. Sponsoring Agency Code

15. Supplementary Notes

16. Abstract

The classic slotted-wall boundary-condition coefficient for rod-wall wind tunnels is derived by approximating the potential flow solution through a cascade of two staggered rows of rods. A comparison with the corrected Chen and Mears solution for flow through an unstaggered cascade is made.

17. Key Words (Suggested by Author(s))	18. Distribution Statement
Wind tunnels Slotted walls Rod walls Boundary-condition coefficient	Unclassified - Unlimited Subject Category 02

19. Security Classif. (of this report)	20. Security Classif. (of this page)	21. No. of Pages	22. Price
Unclassified	Unclassified	20	A02

National Aeronautics and
Space Administration

Washington, D.C.
20546

Official Business
Penalty for Private Use, $300

THIRD-CLASS BULK RATE

Postage and Fees Paid
National Aeronautics and
Space Administration
NASA-451

U.S.MAIL

NASA

POSTMASTER: If Undeliverable (Section 158 Postal Manual) Do Not Return